nature neuroscience

Explicit memory creation during sleep demonstrates a causal role of place cells in navigation

Gaetan de Lavilléon[1–3], Marie Masako Lacroix[1–3], Laure Rondi-Reig[2,4] & Karim Benchenane[1,2,4]

Hippocampal place cells assemblies are believed to support the cognitive map, and their reactivations during sleep are thought to be involved in spatial memory consolidation. By triggering intracranial rewarding stimulations by place cell spikes during sleep, we induced an explicit memory trace, leading to a goal-directed behavior toward the place field. This demonstrates that place cells' activity during sleep still conveys relevant spatial information and that this activity is functionally significant for navigation.

The hippocampus constitutes the neuronal substrate of the cognitive map[1], as demonstrated by the firing of its principal cells in specific locations of the environment[1]. During sleep, hippocampal neurons replay previous wake experiences during so-called sharp wave ripples (SPW-Rs)[2,3], an oscillatory pattern supporting memory consolidation[4–6]. However, while the animal is awake, it is impossible to dissociate its actual position from the associated neuronal firing, and the proposed function of place cells in navigation is based entirely on this correlation[7,8]. We hypothesized that the transient decorrelation of place cell activity from current location during sleep could provide a way to directly test the function of place cells in navigation.

In this study, we used the spontaneous activity of a given place cell during sleep to trigger automatically rewarding stimulations of the medial forebrain bundle (MFB) to create an artificial place–reward association. This version of a closed-loop-based learning procedure[9–12] (**Fig. 1** and **Supplementary Fig. 1**) is similar to the classical place preference task, thought to rely on a form of hippocampus-dependent explicit memory[13].

Mice were implanted with polytrodes in the CA1 pyramidal layer and stimulation electrodes in the MFB (Online Methods), known to induce reward in mice[14,15]. Optimal rewarding intensity was determined in a classical nose-poke procedure (Online Methods). At the intensities used, stimulations neither awakened the animals (**Supplementary Fig. 2**) nor altered basic hippocampal electrophysiological properties, such as place cell characteristics, theta oscillations or SPW-Rs (**Supplementary Figs. 3** and **4**).

As mice freely explored open field environments, spiking activity was analyzed online to determine whether a single and clearly identifiable putative pyramidal neuron displayed a place field (PF, Online Methods and **Supplementary Fig. 1**). Once selected, this place cell was used to trigger MFB rewarding stimulations (2-ms delay) during either the wake-pairing or the sleep-pairing protocol (Online Methods and **Supplementary Figs. 1** and **5**). Exploration was quantified by successive trials in PRE and POST sessions to identify exploratory bias toward the related PF.

The pairing protocol was performed during wakefulness on a first set of five animals (**Fig. 2a** and **Supplementary Fig. 1a**). During the PRE session, spatial behavior was what was expected from a random and homogeneous exploration: the percentage of time mice spent in the PF corresponded to the percentage of the environment occupied by this PF (**Fig. 2b** and **Supplementary Fig. 6**). During the wake-pairing session, mice stayed preferentially in the PF of the selected neuron to self-stimulate, as revealed by the high correlation between place cell firing map and occupancy map (**Fig. 2e** and **Supplementary Fig. 7**). During the POST period, time spent within the PF increased 4- to 5-fold compared to PRE, emphasizing the persistence of the memory of the place–reward association (**Fig. 2a**,**b**, $n = 5$, $P = 0.043$).

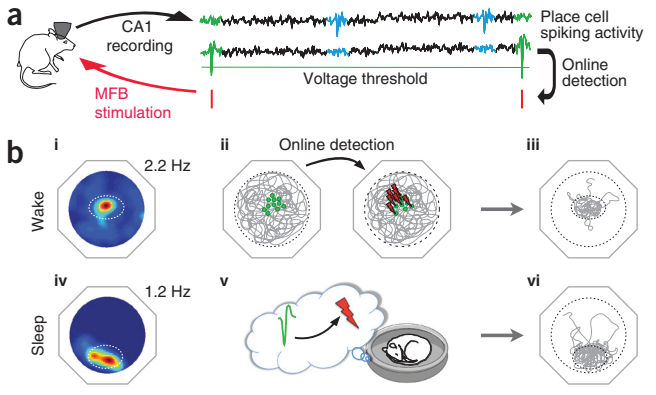

Figure 1 Pairing place cell to rewarding stimulation during wakefulness or sleep to create a place preference. (**a**) Method of online spike detection based on voltage threshold. Schematic waveforms from two units (blue and green) superimposed on signals recorded from hippocampal CA1 pyramidal layer (black). Spikes with high amplitude, crossing the threshold, trigger MFB stimulation. (**b**) Protocol for the creation of a place preference by pairing spikes to rewarding stimulations during wakefulness or sleep. (**i**,**iv**) PFs of selected pyramidal cells. (**ii**) During the pairing protocol performed during wakefulness, spikes of the detected place cell (green circles indicate mouse position when place cell fired) automatically trigger rewarding stimulations (red lightning bolts). (**v**) During sleep pairing, reactivation-related spiking activity of the selected place cell triggers rewarding stimulations. (**iii**,**vi**) Place preference is assessed by probe tests.

[1]Team Memory, Oscillations and Brain States (MOBs), Brain Plasticity Unit, CNRS UMR 8249, Ecole Supérieure de Physique et de Chimie Industrielles de la Ville de Paris, Paris, France. [2]Neuroscience Paris Seine, Cerebellum, Navigation and Memory Team, CNRS UMR 8246; INSERM, UMR-S 1130; Sorbonne Universités, University Pierre and Marie Curie, Paris, France. [3]These authors contributed equally to this work. [4]These authors jointly directed this work. Correspondence should be addressed to K.B. (karim.benchenane@espci.fr).

Received 29 July 2013; accepted 9 February 2015; published online 9 March 2015; doi:10.1038/nn.3970

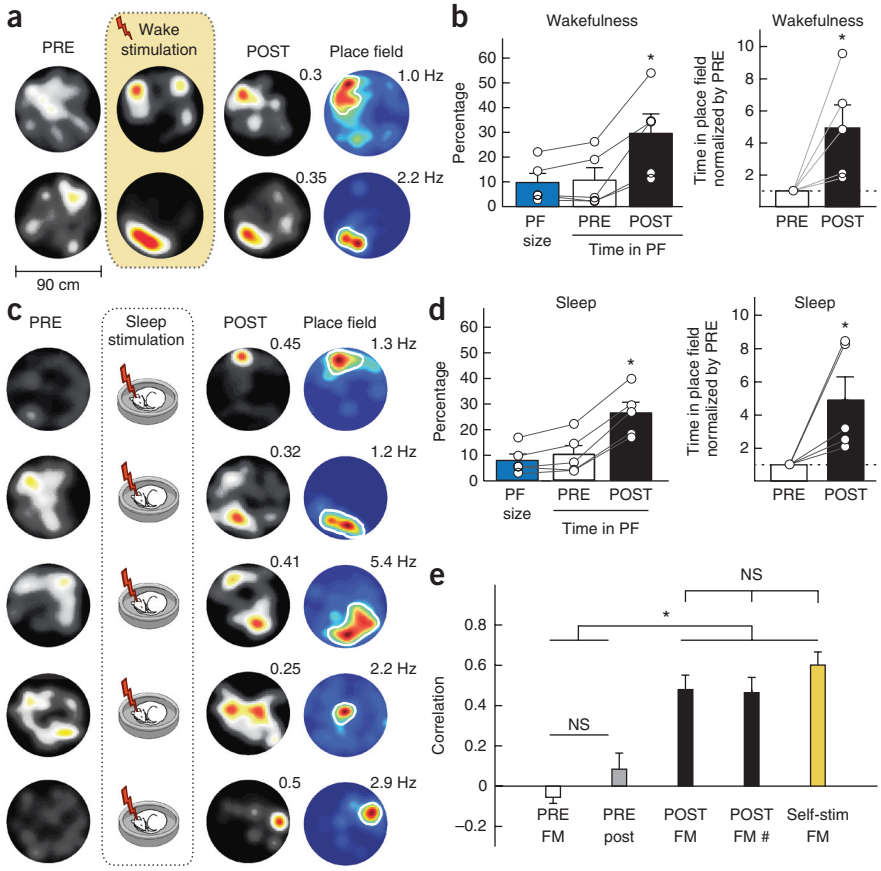

Figure 2 Place preference induced after pairing place cell spikes with rewarding stimulation. (**a**,**c**) Occupancy maps before (PRE), during (**a**, wake stimulation) and after (POST) the session where one place cell's spikes triggered MFB stimulations, either during wakefulness (**a**, representative examples) or sleep (**c**, $n = 5$). Color ranges from black (minimum occupancy rate) to red; peak occupancy rates are indicated above POST occupancy maps, with same scaling applied as for PRE. Corresponding firing maps (FM) of detected place cells before PRE session are represented on the right. Color ranges from blue (minimum firing rate) to red; peak firing rates indicated above. (**b**,**d**) Left, PF size expressed as a percentage of the total reachable area (blue) and percentage of time spent within the PF in PRE and POST sessions. Right, data normalized by PRE sessions after wake-pairing (**b**, PRE/POST, Wilcoxon matched pairs test, $n = 5$, $Z = 2.02$, $^*P = 0.043$) or sleep-pairing protocol (**d**, PRE/POST, $n = 5$, $Z = 2.02$, $^*P = 0.043$). (**e**) Correlation between occupancy maps or correlation between detected place cell's FM and occupancy map, either during PRE and POST sleep-pairing session or during wake-pairing (self-stim) sessions (Friedman test, chi-squared: $\chi^2 = 16.60$, $n = 5$, d.f. = 4, $^*P = 0.0023$). Correlation with FM is increased during POST ($n = 5$, Wilcoxon matched pairs test: correlation PRE–FM versus POST–FM, $Z = 2.02$, $^*P = 0.043$; correlation PRE–POST versus POST–FM, $Z = 2.02$, $^*P = 0.043$). Same results were observed for partial correlation (#), which quantifies the correlation between POST and FM when the influence of PRE is removed ($n = 5$, correlation PRE–FM versus POST–FM given PRE, $Z = 2.02$, $^*P = 0.043$; correlation POST–FM versus POST–FM given PRE, $Z = 0.73$, $P = 0.46$). ($n = 5$, PRE–FM versus self-stimulation–FM, $Z = 2.02$, $^*P = 0.043$; POST–FM versus self-stimulation–FM, $Z = 1.75$, $P = 0.07$). Note the absence of correlation in PRE sessions, excluding a bias of behavior induced by arena properties. NS, not significant (PRE–FM versus PRE–POST, $Z = 0.94$, $P = 0.34$; POST–FM or POST–FM# versus self-stim–FM, $Z = 1.75$, $P = 0.07$). Error bars indicate s.e.m.

The place preference created directly using place cell activity was similar to classical place preference, induced by manual stimulations restricted to a given location (**Supplementary Fig. 8b**,**c**).

A second set of five animals then underwent the pairing protocol during sleep (**Fig. 2c** and **Supplementary Fig. 1b**). Analysis of the POST exploration upon awakening revealed a strong place preference for the associated PFs: the time the animals spent in these locations increased by 4- to 5-fold (**Fig. 2c**,**d**, $n = 5$, $P = 0.043$). Other behavioral measures yielded similar results (**Supplementary Fig. 9**).

During the 1-h sleep-pairing sessions, most of the MFB stimulations occurred during slow-wave sleep (SWS; 567 ± 80) rather than rapid eye movement sleep (REM; 11 ± 7 stimulations). Within SWS periods, 37.4 ± 8.9% occurred during SPW-Rs, which represented only 1.43 ± 0.2% of total sleep. This is consistent with the large increase in firing rate during SPW-Rs and with the hypothesis that SPW-Rs are essential for memory consolidation during sleep[5,6]. Since very few REM episodes were observed during these short sleep sessions, however, further studies would be needed to test whether this effect depends on a particular sleep stage.

Observation of animals' trajectories during POST trials of the sleep-pairing protocol suggested that mice headed directly toward the PF (**Fig. 3a**). Accordingly, the time of first entry into the PF was significantly decreased in POST compared to PRE sessions. (**Fig. 3a**, $n = 5$, $P = 0.043$). All behavioral measures tended to show an increased exploration of the selected PFs during the first two trials after the sleep learning procedure when compared to the third and fourth trials, consistent with an extinction classically observed during unrewarded probe tests (**Fig. 3b**, Online Methods). Notably, the same pairing protocol during sleep with non-rewarding MFB stimulations (those that did not lead to self-stimulating behavior) did not induce any subsequent place preference upon awakening (**Fig. 3c**). Moreover, we found a significant correlation between the learning induced by the sleep-pairing protocol (an increase of time spent within the PF) and the rewarding effect of MFB stimulation ($n = 7$, $r = 0.85$, $P = 0.01$, **Fig. 3c**), assessed by self-stimulation in a subsequent control wake-pairing session (Online Methods). Finally, there was no modification of the number of place cell–triggered MFB stimulations over time during the sleep-pairing session (**Supplementary Fig. 2e**), excluding an operant conditioning of the driving neuron, a phenomenon observed in other cellular conditioning studies[9,10,12].

Taken together, these observations fulfill criteria proposed by Dickinson and Balleine to define a goal-directed strategy based on explicit knowledge of action–outcome association[16]. This suggests that the pairing protocol used here during sleep induced the creation of an artificial explicit memory that could be used by mice in a goal-directed way and thus goes beyond previous observations showing that certain forms of conditioning relying on a reflex response to a conditioned stimulus can take place in the sleeping or anesthetized brain[17–19]. Moreover, the fact that pairing spikes of a given place cell with rewarding stimulation during sleep, when its activity was decorrelated from the actual animal position, leads to a place preference toward the related place field demonstrates that place cell activity

Figure 3 Pairing MFB stimulations to place cell activity during sleep leads to a goal directed behavior upon awakening. (**a**) Left, firing map of the detected place cell and trial-by-trial trajectories for the POST session of the first example shown in **Figure 2c**. Right, quantification of the delay to reach the PF for the first time, showing a significant decrease in POST compared to PRE sessions (Wilcoxon matched pairs test, $n = 5$, $Z = 2.02$, $^*P = 0.043$). (**b**) Analysis comparing the first (1 and 2) and last (3 and 4) trials of the PRE and POST sessions of the sleep-pairing protocol, on time of first entry into PF ($n = 5$, trials 1 and 2: $Z = 2.02$, $^*P = 0.043$; trials 3 and 4: $Z = 0.94$, $P = 0.34$), cumulative distance (A.U., arbitrary units) to the PF ($n = 5$, trials 1 and 2: $Z = 2.02$, $^*P = 0.043$; trials 3 and 4: $Z = 1.48$, $P = 0.14$) and percentage of time spent in PF ($n = 5$, trials 1 and 2: $Z = 2.02$, $^*P = 0.043$; trials 3 and 4: $Z = 1.75$, $P = 0.07$). (**c**) Left and middle, time spent in PF in PRE (white bar) and POST (black) sessions of the sleep-pairing protocol and during self-stimulation session of the control wake protocol (green) for all mice ($n = 7$), including mice without self-stimulating behavior (purple dots; exclusion criterion 3). Friedman test, $\chi^2 = 12.28$, $n = 7$, d.f. = 2, $P = 0.021$; Wilcoxon matched pairs test, $n = 7$, PRE–POST sleep-pairing: $Z = 2.36$, $^*P = 0.017$; PRE–POST wake-pairing: $Z = 2.36$, $^*P = 0.017$; POST–control wake-pairing: $Z = 2.19$, $^*P = 0.028$. Right, correlation between the increase in time spent in PF during control wake self-stimulation protocol and upon awakening after sleep pairing. Spearman correlation, $n = 7$, $r = 0.85$, $t_5 = 3.72$, $^*P = 0.01$. Learning index refers to difference in percentage of time in PF, between PRE sessions and POST or during control wake self-stimulation. Error bars indicate s.e.m.

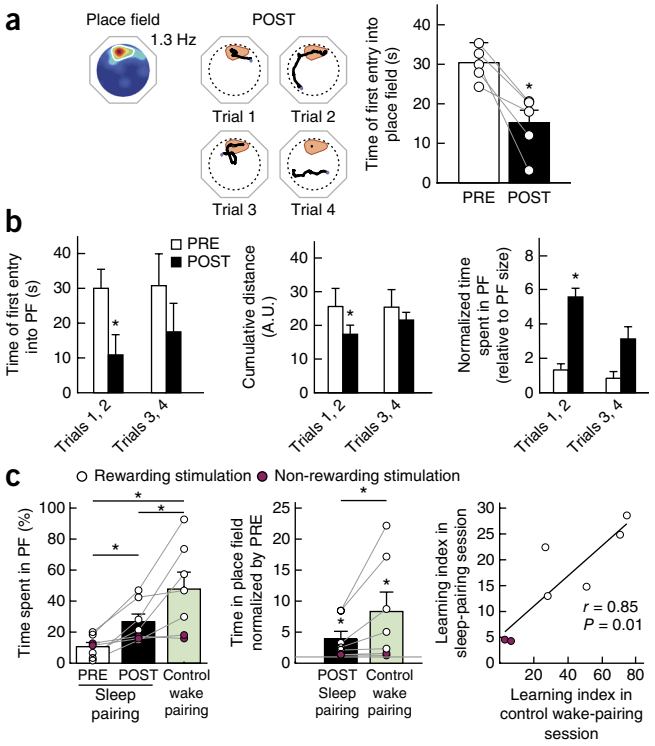

itself functions in spatial memory and navigation. Finally, our results support the theory of spatial reactivation during sleep[3,4,20] by showing that place cells encode the same spatial information during sleep and wakefulness.

METHODS

Methods and any associated references are available in the online version of the paper.

Note: Any Supplementary Information and Source Data files are available in the online version of the paper.

ACKNOWLEDGMENTS

We thank F.P. Battaglia, M.B. Zugaro, P. Faure, L. Roux, S. Bagur and S.I. Wiener for discussions, and A. Peyrache for discussion and critical readings of an earlier version of the manuscript. Some experiments were done with software developed by G. Cournelle and A. Baelde, engineering students from the ESPCI-ParisTech. This work was supported by the Fondation pour la Recherche Médicale DEQ20120323730, France, by the National Agency for Research ANR-REG-071220-01-01, France, by the CNRS: Programmes Interdisciplinaires de Recherche (Neuro-IC), ATIP-Avenir (2014) and by the city of Paris (Grant Emergence 2014). This work also received support under the program Investissements d'Avenir launched by the French Government and implemented by the ANR, with the references: ANR-10-LABX-54 MEMO LIFE and ANR-11-IDEX-0001-02 PSL* Research University. G.d.L. and M.M.L. were funded by the Ministère de l'Enseignement Supérieur et de la Recherche, France.

AUTHOR CONTRIBUTIONS

K.B. designed the experiment. G.d.L. and M.M.L. did the experiments. K.B., G.d.L. and M.M.L. analyzed the data. K.B., G.d.L., M.M.L. and L.R.-R. wrote the manuscript.

COMPETING FINANCIAL INTERESTS

The authors declare no competing financial interests.

1. O'Keefe, J. & Nadel, L. *The Hippocampus as a Cognitive Map* 1–570 (Oxford University Press, 1978).
2. Lee, A.K. & Wilson, M.A. *Neuron* **36**, 1183–1194 (2002).
3. Wilson, M.A. & McNaughton, B.L. *Science* **265**, 676–679 (1994).
4. Buzsáki, G. *Neuroscience* **31**, 551–570 (1989).
5. Girardeau, G., Benchenane, K., Wiener, S.I., Buzsáki, G. & Zugaro, M.B. *Nat. Neurosci.* **12**, 1222–1223 (2009).
6. Ego-Stengel, V. & Wilson, M.A. *Hippocampus* **20**, 1–10 (2010).
7. Lenck-Santini, P.-P., Muller, R.U., Save, E. & Poucet, B. *J. Neurosci.* **22**, 9035–9047 (2002).
8. Jeffery, K.J., Gilbert, A., Burton, S. & Strudwick, A. *Hippocampus* **13**, 175–189 (2003).
9. Delgado, J.M.R., Johnston, V.S., Wallace, J.D. & Bradley, R.J. *Brain Res.* **22**, 347–362 (1970).
10. Shinkman, P.G., Bruce, C.J. & Pfingst, B.E. *Science* **184**, 1194–1196 (1974).
11. Jackson, A., Mavoori, J. & Fetz, E.E. *Nature* **444**, 56–60 (2006).
12. Fetz, E.E. *Science* **163**, 955–958 (1969).
13. Eichenbaum, H. *Behav. Brain Res.* **103**, 123–133 (1999).
14. Carlezon, W.A. & Chartoff, E.H. *Nat. Protoc.* **2**, 2987–2995 (2007).
15. Kobayashi, T., Nishijo, H., Fukuda, M., Bures, J. & Ono, T. *J. Neurophysiol.* **78**, 597–613 (1997).
16. Dickinson, A. & Balleine, B.W. *Anim. Learn. Behav.* **22**, 1–18 (1994).
17. Hennevin, E. & Hars, B. *Psychobiology (Austin, Tex.)* **20**, 166–176 (1992).
18. Weinberger, N.M., Gold, P.E. & Sternberg, D.B. *Science* **223**, 605–607 (1984).
19. Arzi, A. *et al. Nat. Neurosci.* **15**, 1460–1465 (2012).
20. Pavlides, C. & Winson, J. *J. Neurosci.* **9**, 2907–2918 (1989).

ONLINE METHODS

Subjects and surgical protocols. A total of 40 C57Bl6 male mice (*Mus musculus*), 3–6 months old, were implanted with movable polytrodes (six or eight twisted nichrome wires) above the CA1 pyramidal layer of right hippocampus (AP +2.2, ML +2.0, DV −1.0). Stimulation electrodes (60-µm-diameter stainless steel) were implanted at the left medial forebrain bundle (MFB) (AP +1.4, ML +1.2, DV +4.8). During recovery from surgery (minimum 3 d) and during all experiments, mice received food and water *ad libitum*. The recording electrodes were progressively lowered until they reached the CA1 pyramidal layer, where ripples were recorded. Meanwhile, the mice were habituated to explore three different open fields. All mice were free of any manipulation before being included in this study. Mice were housed in an animal facility (08:00–20:00 light), one per cage after surgery. Data collection and analysis were not performed blind to the condition of the experiments, and no randomization was used. All behavioral experiments were performed in accordance with the official European guidelines for the care and use of laboratory animals (86/609/EEC) and in accordance with the Policies of the French Committee of Ethics (Decrees n° 87–848 and n° 2001–464). Animal housing facility of the laboratory where experiments were made is fully accredited by the French Direction of Veterinary Services (B-75-05-24, 18 May 2010). Animal surgeries and experimentations were authorized by the French Direction of Veterinary Services for K.B. (14-43) and L.R.-R. (75-752).

Electrophysiological procedures. *Recordings.* Signals from all electrodes were fed into a unity-gain headstage preamplifier (HS-16; Neuralynx, Bozeman, MT) and then amplified 2,000 times (tether cable to programmable amplifiers Lynx8, Neuralynx, Bozeman, MT). Signals for single-unit recordings were bandpass-filtered between 600 and 9,000 Hz. Data were digitized and stored on hard disk by a Power 1401 (CED, Cambridge, UK) acquisition system controlled by Spike2 software (CED, Cambridge, UK). Single-unit data were sampled at 20 kHz and 1.6-ms samples were time-stamped and stored for all channels of the polytrode whenever any of the channels exceeded a preset threshold. Local field potentials were sampled and stored at 1,250 Hz. During exploration or sleep recording sessions, mice were tracked by video at 30 Hz and position of the animals was reconstructed by a Matlab-based program (MathWorks, Natick, MA).

MFB stimulations. Intracranial rewarding stimulation consisted of a stimulation train lasting 100 ms and composed of 14 1-ms negative square-wave pulses (140 Hz)[21]. Optimal voltage for intracranial MFB was determined with a nose-poke task (see below). Note that these MFB stimulations did not reset theta oscillations, an effect that has been observed in some studies with stimulations located in the hypothalamic area[22,23].

Nose-poke task. In the nose-poke task, the rodent self-administered electrical brain stimulations in an operant chamber (50 × 30 × 20 cm) with one panel composed of two 1.5-cm-diameter holes, in a daily session for 3 d. Each nose-poke into the left hole was detected by a photodetector and automatically triggered MFB stimulations. Mice were screened for decreasing voltage of stimulations from 8 V to 0 V in 200-s sessions. Percentage of time spent on self-stimulation was modulated by voltage intensity in accordance with previous report[21]. For subsequent experiments of place-reward association, we then used for each mouse the lowest stimulation intensity necessary to reach at least 80% of its time nose-poking while having no effect on sleep. Four mice did not show any self-stimulating behavior in this task and were thus excluded from the study (exclusion criterion 1).

Place preference tasks. *Common paradigm.* Mice were habituated to freely explore during daily 30-min sessions three distinct open fields (120 cm diameter), whose shape was either circular, square or star-shaped and surrounded by different cues. Exploration area was restricted by the length of the recording cable and all occupancy maps thus correspond only to the circular reachable area. This procedure did not affect quality of recording and was chosen to improve homogeneity of exploration as compared to that in a classical open field surrounded by walls (**Supplementary Fig. 10**).

Our place preference task started with a PRE session consisting of eight successive 1-min exploration trials. Then, during a pairing session, either place cell activity (sleep-pairing or wake-pairing protocols) or animal entry into a defined location (classical place preference) triggered MFB rewarding stimulations. This session was directly followed by a POST probe test, consisting of successive 1-min exploration trials (**Supplementary Fig. 1**). As we were aiming to quantify a putative place preference, quantifications of PRE and POST sessions were done using the first four trials during which the mouse was actively exploring; trials during which mice stayed in the starting zone (within a 10-cm diameter) were not considered for the analysis. Regarding this criterion, in the sleep-pairing protocol 0.28 ± 0.18 PRE trials and 1.71 ± 0.28 POST trials per mouse were removed from analysis. In the wake-pairing protocol, 0.2 ± 0.2 PRE trials and 0.6 ± 0.4 POST trials were removed.

During PRE and POST sessions, a different starting point among four locations was assigned to each trial to force mice to use external visual cues for navigation (an allocentric strategy, known to depend on hippocampal integrity[24]). For each experiment, the four starting points were set symmetrically at the edge of the exploring area (**Supplementary Fig. 1d**). None of the starting points was located inside the PF, and the first trial started at the opposite side of the arena from the PF. The three remaining locations were then sequentially visited. Between trials, mice were removed from the environment and carried to the next starting point (~5-s intertrial interval).

All experiments were performed during daytime (12:00–15:00) unless specified in order to favor sleep in the sleep-pairing experiment. The behavioral task, however, was not sensitive to circadian rhythm (**Supplementary Fig. 8c–f**).

Wake-pairing protocol (using place cell activity). During the wake-pairing protocol, place cell spikes were paired with MFB stimulation at the rewarding intensity during a free exploration session, lasting 15 min after the first stimulation. The experiment was performed when spikes of a putative pyramidal cell could be efficiently and unambiguously detected online and when the corresponding PF was unique and salient (see Online Methods, "Online spike detection"). Five animals performed this wake-pairing protocol.

Sleep-pairing protocol (using place cell activity). The experiment was performed when spikes of a putative pyramidal cell reached the online spike detection criteria, and 24 of the implanted mice were therefore excluded from the study before even experiencing the sleep-pairing protocol (criterion 2). During the sleep-pairing protocol, spikes of the selected place cell were paired with MFB stimulation during 1 h of sleep. Mice slept in their home cages, which were placed outside the exploring arena and surrounded by opaque paper. An experimenter stopped the online pairing when the animal spontaneously woke up (movements seen on real-time video and decrease of the delta band in the online spectrogram). Offline analysis confirmed that the stimulation train did not modify sleep spectrograms (**Supplementary Fig. 2**) nor the occurrence of SPW-Rs (**Supplementary Fig. 4c**). Mice experienced no place preference task before the sleep-pairing protocol.

Control wake-pairing protocol (using place cell activity). The nose-pose task used to quantify the rewarding effect of MFB stimulations was done several days before the sleep-pairing protocol. It was thus important to confirm that the MFB stimulation was still rewarding at the time of the experiment. Just after the sleep-pairing protocol, efficiency of rewarding stimulations was always evaluated during a control wake-pairing protocol. These control sessions were preceded by a period of free exploration of the environment (30 min) to induce full extinction of the putative memory trace. Two mice performed the protocol with unrewarding stimulation and were therefore excluded from the main analysis (exclusion criterion 3). All other variables for these two animals were identical otherwise (**Supplementary Fig. 2**).

Classical place preference task (manual stimulations in an area defined by experimenter). Seven animals experienced a classical place-reward association during free exploration of the arena during light phase (12:00–15:00) and five of them experienced an ulterior session (with a different rewarded location) during dark phase (00:00–03:00). Mouse position was tracked in real time with a video camera and rewarding stimulations were delivered when mice reached a pre-established area, covering around 5% of the total surface of exploration (**Supplementary Fig. 8c,d**).

Exclusion criteria for behavioral experiments. As previously mentioned, 4 implanted mice were excluded because MFB stimulations did not induce self-stimulating behavior in the nose-poke task (criterion 1), 24 because they did not fulfill the criteria for online spike sorting or PF properties (criterion 2), and 2 because they did not show any self-stimulating behavior in the control wake-pairing session following the sleep-pairing protocol (criterion 3; see "Quantification of place preference at the single-mouse level").

doi:10.1038/nn.3970

Offline spike sorting. Extracted waveforms were sorted via a semiautomatic cluster cutting procedure using KlustaKwik[25] and Klusters[26] (http://neurosuite.sourceforge.net/). Recordings were visualized and processed using NeuroScope and NDManager (http://neurosuite.sourceforge.net/). Isolation distance was computed with parameters proposed by Schmitzer and colleagues[27]. Since this measure depends on the number of channels, isolation measures were computed with only four of the recording channels and compared with recommended values (given for tetrode recordings). All neurons displayed isolation distance above 25 for the wake-pairing protocol and 42 for the sleep-pairing protocol, values considered as good isolation by Schmitzer and colleagues (mean isolation distance: 86 ± 23, $n = 10$)[27].

Online spike detection triggering MFB stimulations. Since the seminal work by Fetz and colleagues[28–31], closed-loop systems between neural activity and either reward or electrical stimulation have been used to induce learning or to study plasticity. Yet there is still no consensus regarding the most accurate method for online spike sorting. Spikes were detected online by a simple voltage threshold applied on one specific channel of a polytrode (signal filtered above 600 Hz, referenced to a local channel without spiking activity) by a custom program in Spike2 software. This threshold was manually adjusted to detect only the highest action potentials, and the use of hexa/octrodes instead of tetrodes enhanced the probability of being in this situation. Waveforms of the detected spikes, averaged online in Spike2, allowed us to distinguish narrow spikes (usually interneuron) from large ones coming from a putative pyramidal cell. The presence of complex spikes further supported an origin from a putative pyramidal cell, and a comparison of the waveforms of all channels observed online supported detection of only one neuron (later confirmed by offline clustering). The experimenter then checked, with help of a homemade Matlab program displaying a firing rate map (FM) in real time, whether the detected putative pyramidal neuron displayed a place field. When a place cell had been detected with a given threshold, this latter was then used to automatically trigger MFB stimulation through a brain-computer interface with a delay less than 2 ms. A refractory period of 1 s from train onset was added to prevent the induced electrical artifact from being detected when crossing the threshold, leading to further stimulation not related to real spiking activity.

The quality of the online spike sorting was confirmed by comparison with offline spike sorting in terms of sensitivity and specificity (**Supplementary Fig. 5**). On average, the online spike sorting system allowed the detection of $52.9 \pm 9.5\%$ of the spikes of a single pyramidal neuron as assessed by an offline spike sorting procedure, consistent with the proportion of complex spikes that do not reach the voltage threshold[32]. During a sleep session, all spikes detected online were followed by the stimulation. Yet in spite of the electrical artifact due to stimulations, spikes were still detected by offline spike sorting, showing that $43.2 \pm 10.9\%$ of spikes were followed by stimulations during the sleep-pairing protocol. Overall, this shows that the detection method is highly specific, with very few false-positive detections—our main objective—but with lower sensitivity, which was not a crucial factor for our experiment.

Electrophysiological and behavioral analysis. Analyses were performed with custom-made Matlab programs, based on generic code that can be downloaded at http://www.battaglia.nl/computing/ and http://fmatoolbox.sourceforge.net/.

Occupancy maps. For each exploration session, spatial density of raw trajectories in the circular reachable area was computed, normalized and smoothed. Occupancy rates thus correspond to the ratio of session time spent at a particular bin (sum of all values distributed over bins equals 1). For PRE and POST sessions composed of four trials, the same results were obtained when averaging the four maps of the successive trials, as well as when computing the map of the concatenated trajectories from those trials.

Place field analysis. A place field (PF) was defined as an area with more than nine adjacent pixels displaying a firing rate above the mean firing rate of the neuron[33]. The limits of the PF were then estimated by using the smoothed rate map corresponding to the area with a firing rate above 50% of the peak firing rate within the PF. To control for border effect due to our definition of the PF, behavioral analyses were also done in an increased area, referred to as "large place field," done with the Matlab function "imdilate" (**Supplementary Fig. 9a**), as classically done in Morris water maze experiments[34].

Stability of the PF and efficiency of wake stimulations was determined by correlation analyses obtained by the bin-by-bin correlation coefficient between two different FMs or between FM and occupancy map. Partial correlation analyses were done with the function "partialcorr" in Matlab (**Fig. 2e** and **Supplementary Fig. 7**).

Behavior. Several measures were used to quantify exploration: time to enter the PF for the first time, cumulative distance defined as the instantaneous distance between the mouse position and PF center of mass, percentage of time spent within PF, and smoothed occupancy map obtained from raw trajectories. To quantify the learning effect of the pairing procedures, different normalizations were used to account for the different size of PFs: normalization by values in the PRE session or normalization by the PF size (**Supplementary Fig. 9b**). All comparisons between PRE and POST gave similar results when looking at ratios (POST/PRE) or differences (POST – PRE). Periods showing grooming behaviors were excluded from the analyses.

Quantification of place preference at the single-mouse level. For this quantification, we first computed the theoretical time spent in the PFs excepted by chance; that is, 10% of total exploration time spent in a PF representing 10% of the total reachable area (24 s out of 240 s corresponding to 4 trials lasting 60 s each). This was then compared to the observed proportion of time spent inside and outside the PF in the PRE session with a chi-squared test. This showed that exploration in PRE session was similar to that expected by chance. A similar chi-squared test comparison was done between PRE and POST session and between PRE and self-stimulating session in the control wake experiment. This latter analysis was used to exclude mice that did not show self-stimulating behavior in the control wake session (criterion 3).

We also computed a theoretical distribution of time spent in the PFs by using all trajectories of the PRE sessions (before any learning) taken from experiments in all protocols. As we analyzed only the first four trials in this study, one combination of four trials among the available PRE trials was assessed for each experiment. We computed the percentage of time spent in the five different PFs of the sleep protocol, for all obtained combinations except when the starting point was located within the selected PF ($n = 5{,}914$ values). This percentage was then normalized by the respective size of each PF and used to create the distribution corresponding to random exploration (**Supplementary Fig. 6c**).

Sleep scoring. To determine sleep periods, a 30-Hz camera placed 30 cm above the cage videotaped the mouse. Frame-by-frame image difference allowed determining sensitively the movements of the animal; the immobility threshold was set above respiratory movements. Sleep stages were determined by automatic *k*-means clustering of the theta/delta ratio extracted from the power spectrograms of hippocampal LFP signal during the episodes where the animal was immobile. REM sleep corresponded to high theta/delta ratio periods, SWS to low ratio periods.

Sharp-wave ripple detection. Offline ripple detection was performed by band-pass filtering (100–250 Hz), squaring and normalizing the field potential recorded in CA1 pyramidal layer. Ripples were defined as events peaking above 5 s.d. The beginning and end of a SPW-R were defined with a threshold of 3 s.d.

Peri-event histograms (PETHs) were calculated for the rate of spikes (in hertz) with reference to the deepest trough of all detected SPW-Rs. To compare the results between PETH centered to spike-triggered stimulation and PETH centered to SPW-Rs, a 5-ms jitter was added in the latter condition to account for the synchronization effect induced by the alignment of all ripples to the same phase, corresponding to the deepest trough (**Supplementary Fig. 4g–i**).

To detect the percentage of stimulation occurring during ripples, the same analysis was done on the 70 ms before the stimulation (after removing the stimulation artifact). The signal was filtered between 100 and 250Hz, squared and normalized, and we used the threshold identified by 3 s.d. obtained on stimulation-free periods. Presence of ripples was confirmed when the root mean square remained above the threshold for at least the last 30 ms before the stimulations. Note that this method is likely to underestimate the number of stimulation occurring during ripples if the spikes triggering the stimulation occur at the very beginning of the ripples.

Statistical analysis. Statistical analyses were done by using Matlab (Statistical Toolbox) and Statistica. Because the data did not have a normal distribution, we used non-parametric tests.

Statistical analyses were done with Wilcoxon matched pairs tests on raw and normalized data (by PRE session values or relatively to the PF size). For comparison between different independent groups, we used the Mann-Whitney test. When multiple comparisons were present, *post hoc* group comparisons were always preceded by global analysis: Kruskal-Wallis test for unpaired protocols and Friedman test for paired protocols. In all graphics, error bars correspond to mean ± s.e.m. and asterisks to *P* value ($*P < 0.05$, $**P < 0.01$).

Statistical power is defined as the probability of rejecting the null hypothesis when it is in fact false and should be rejected. We computed the power analysis with a Wilcoxon match paired test, comparing five values taken from a control distribution to five values taken from two different cases of test distributions. In the first situation, the control situation corresponds to five values randomly chosen according to the probability density function displayed in **Supplementary Figure 6** (corresponding to performance related to five real trajectories obtained by the bootstrap procedure described in "Quantification of place preference at the single-mouse level"). Each time, those chosen values were compared to the real performance of the five mice after the sleep-pairing protocol. This was done 1,000 times and only 52 comparisons were not significant, leading to a statistical power of 0.948. In the second situation, the control situation was identical, but the test situation corresponded to a random sampling among a distribution with same mean and variance as the real performance values of the five mice after the sleep-pairing procedure. In that case, the statistical power was 0.798. Note that the same range of statistical power was obtained if we used a control distribution with the mean and variance of the real performance of our five mice during the PRE session (that is, before the sleep-pairing protocols). In this case, the statistical power obtained for the two situations were, respectively, 1 and 0.84. All the statistical powers of our analyses are in the range or above the 0.8 threshold classically used to define powerful statistics. Altogether, this shows that the statistical power of our analyses is strong enough to support the conclusion of our study.

For the evaluation of behavioral extinction of learning, we showed that all behavioral measures used (time spent within PF, cumulative distance, time to first entry) showed a statistical difference between PRE and POST session when considering the first two trials, but not for the last two trials. This observation suggests an extinction of the artificial association created earlier. Nevertheless, it is important to note that this is not a statistical proof. Indeed, the appropriate way to address this question is by testing interaction in a two-way ANOVA, and it has been shown that other analyses can lead to erroneous interpretations[35]. However, our data did not satisfy criteria for parametric tests and there is no consensus concerning a non-parametric test for interaction in a two-way experimental design. Although the effect was observed for all behavioral measures tested, we decided to limit our results interpretation as being consistent with classical extinction.

Histology. After completion of the experiments, mice were deeply anesthetized with ketamine/xylazine solution (10% /1%). With the electrodes left *in situ*, the animals were perfused transcardially with saline (~50 ml), followed by ~50 ml of PFA (4 g/100 mL). Brains were extracted and placed in PFA for postfixation for 24 h, transferred to PBS for at least 48 h, and then cut into 50-µm-thick sections using a freezing microtome and mounted and stained with Cresyl violet. We then visually confirmed that recoding electrodes were implanted in the pyramidal layer of CA1 field and that stimulation electrodes reached the MFB.

A **Supplementary Methods Checklist** is available.

21. Carlezon, W.A. & Chartoff, E.H. *Nat. Protoc.* **2**, 2987–2995 (2007).
22. McNaughton, N. & Sedgwick, E.M. *Neuroscience* **3**, 629–632 (1978).
23. Paxinos, G. & Bindra, D. *Physiol. Behav.* **5**, 227–231 (1970).
24. O'Keefe, J. & Nadel, L. *The Hippocampus as a Cognitive Map* 1–570 (Oxford University Press, 1978).
25. Harris, K.D., Henze, D.A., Csicsvari, J., Hirase, H. & Buzsáki, G. *J. Neurophysiol.* **84**, 401–414 (2000).
26. Hazan, L., Zugaro, M.B. & Buzsáki, G. *J. Neurosci. Methods* **155**, 207–216 (2006).
27. Schmitzer-Torbert, N., Jackson, J., Henze, D., Harris, K. & Redish, A.D. *Neuroscience* **131**, 1–11 (2005).
28. Delgado, J.M.R., Johnston, V.S., Wallace, J.D. & Bradley, R.J. *Brain Res.* **22**, 347–362 (1970).
29. Shinkman, P.G., Bruce, C.J. & Pfingst, B.E. *Science* **184**, 1194–1196 (1974).
30. Fetz, E.E. & Finocchio, D.V. *Science* **174**, 431–435 (1971).
31. Jackson, A., Mavoori, J. & Fetz, E.E. *Nature* **444**, 56–60 (2006).
32. Harris, K.D., Hirase, H., Leinekugel, X., Henze, D.A. & Buzsáki, G. *Neuron* **32**, 141–149 (2001).
33. Muller, R.U., Kubie, J.L. & Ranck, J.B.J. *J. Neurosci.* **7**, 1935–1950 (1987).
34. Maei, H.R., Zaslavsky, K., Teixeira, C.M. & Frankland, P.W. *Front. Integr. Neurosci.* **3**, 4 (2009).
35. Nieuwenhuis, S., Forstmann, B.U. & Wagenmakers, E. *Nat. Neurosci.* **14**, 1105–1107 (2011).

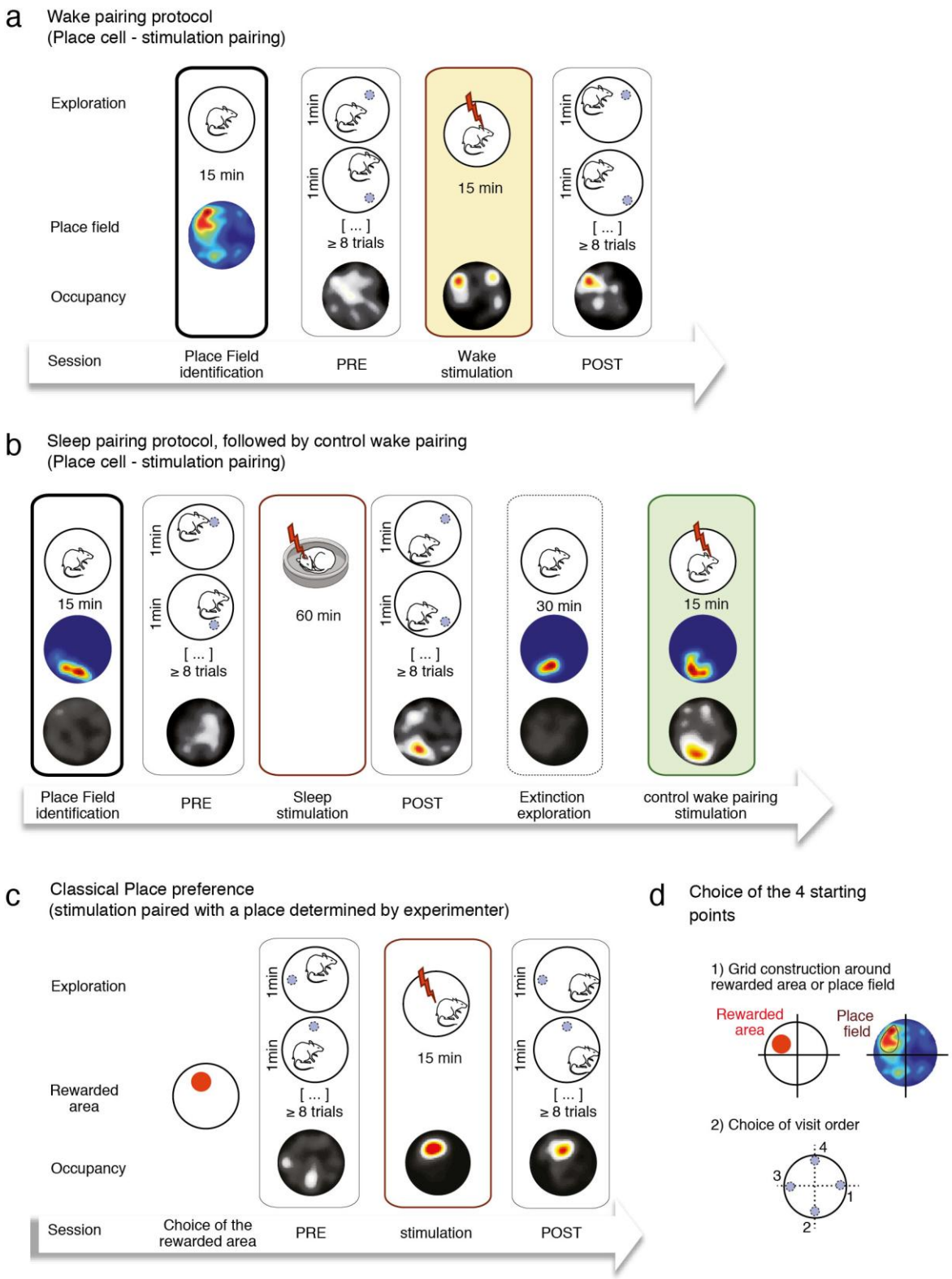

Nature Neuroscience: doi:10.1038/nn.3970

Supplementary Figure 1

The place preference tasks.

a. ***Wake pairing protocol***. The paradigm consisted in four sessions: 1) free exploration and place field identification, 2) basal exploration (PRE), 3) 15 minutes exploration with pairing where online detected spikes of a given place cell triggered MFB stimulation, and 4) test exploration (POST). In PRE and POST session a minimum of eight 60s—trials with changing starting point (gray circles) is performed. Analyses were carried on the first 4 trials where animal was actively exploring. **b**. ***Sleep pairing protocol***. As in panel **a**, the sleep protocol is composed of the same four sessions except that spike—stimulation pairing is performed during 1h of sleep. This protocol was always followed by free exploration to erase the learning (extinction exploration) and a control wake pairing. **c**. ***Classical Place preference task.*** Mouse position was tracked in real time with a video camera during a session lasting 15 minutes. Rewarding stimulations were then delivered when mice reached a pre—established area, covering around 5% of the total surface of exploration. This stimulation phase was preceded by a basal exploration (PRE) and followed by a probe exploration (POST) as described in panel **a**. **d**. Method for the choice of the 4 starting points used in PRE and POST sessions of all place preference paradigms.

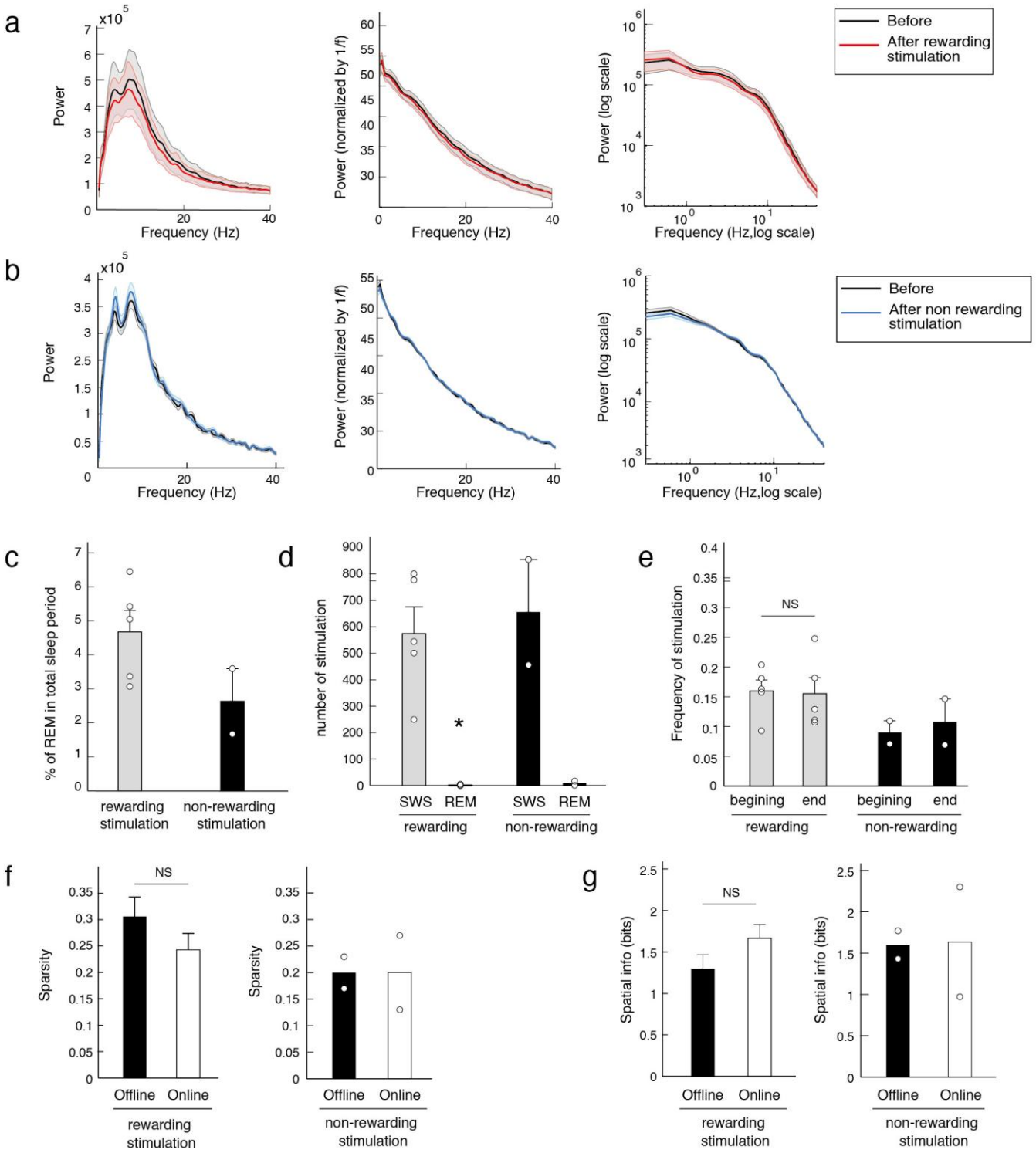

Nature Neuroscience: doi:10.1038/nn.3970

Supplementary Figure 2

Characteristics of sleep pairing sessions with rewarding and non-rewarding MFB stimulations, showing similar properties and absence of sleep perturbation.

a—b. Power spectrum averaged on 3s—period before MFB stimulations train (black), and on 3s period (starting 1s after stimulation train onset to avoid electrical artifact) after rewarding stimulation (**a**, red) or non—rewarding stimulation (**b**, blue) during sleep pairing sessions. From left to right: row power spectrum, spectrum normalized by 1/f and log scaled power spectrum. Colored areas represent SEM. **c**. Percentage of time spent in REM during the total sleep period of the sleep pairing experiment, with either rewarding (grey, n=5) or non—rewarding (black, n=2) stimulations. **d**. Number of stimulation in SWS and REM (Wilcoxon matched pairs test, rewarding condition, n=5, Z=2.02, P=0.043). **e**. Frequency of rewarding and non—rewarding stimulations during the first 10min (beginning) and the last 10min (end) of the sleep pairing sessions (Wilcoxon matched pairs test, rewarding condition, n=5, Z=0.13, P=0.89). This shows that the number of place cell—triggered stimulations is not modified along the pairing protocol, excluding an operant conditioning of the neurons. **f—g**. Sparsity (**f**) and spatial information (**g**) of online and offline detected place cells used to trigger rewarding or non—rewarding stimulations, in sleep and wake—pairing protocols. Wilcoxon matched pairs test, rewarding condition, n=10, f: Z=1.58, P=0.11 ; g: Z=1.27, P=0.20.
* P <0.05 , NS: non significant. Error bars indicate SEM.

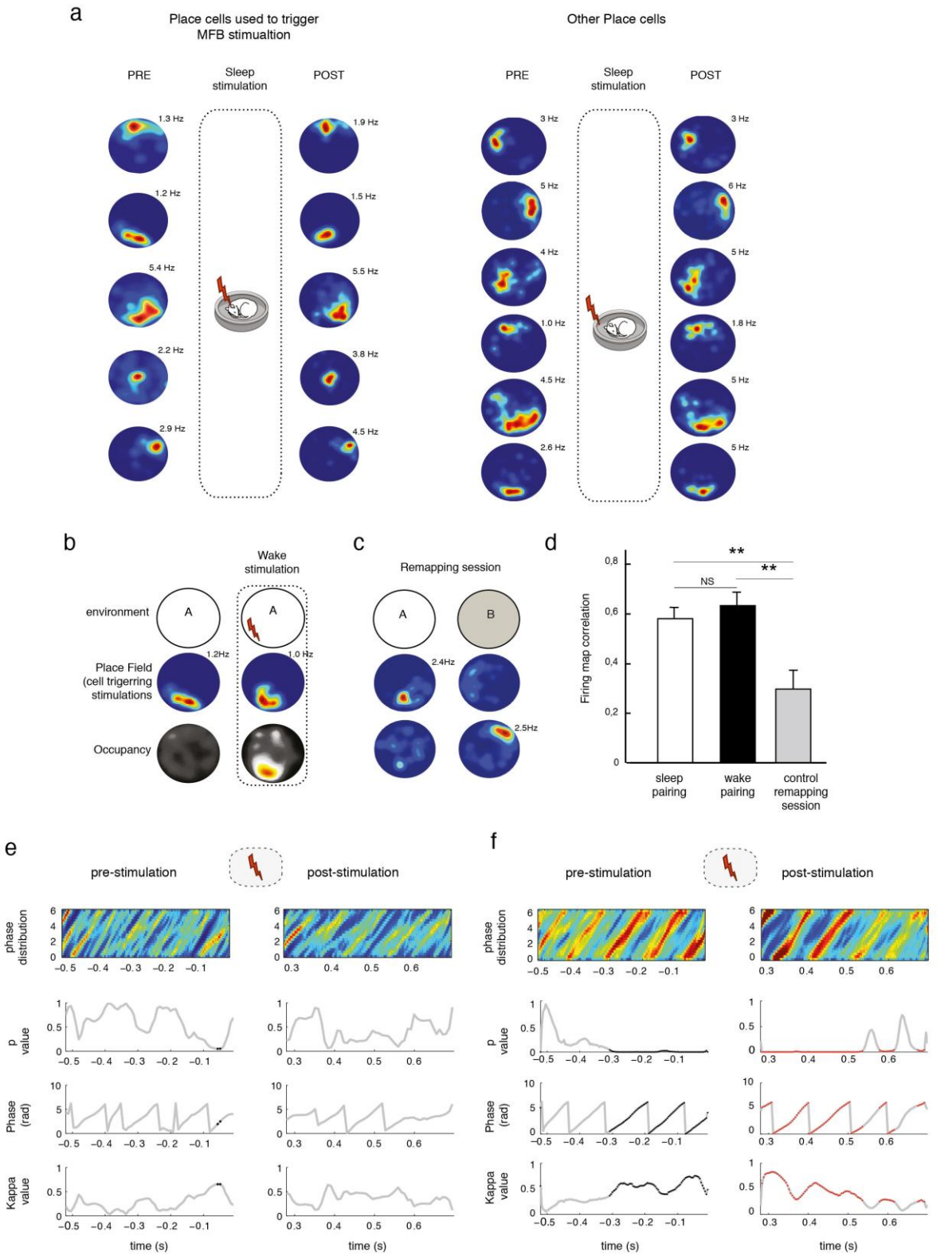

Nature Neuroscience: doi:10.1038/nn.3970

Supplementary Figure 3

Place cells activity and theta oscillations remain stable after MFB stimulations.

a. Place fields of all online detected place cells used to trigger stimulation during sleep (left), and of all other simultaneously recorded place cells (right), during exploration of the same environment before (PRE) or after (POST) the sleep pairing protocol. Color scale indicates firing rate, maximum being indicated above the map. **b**. Firing map and occupancy map before and during the control wake pairing protocol. **c**. Exploration sessions with classical remapping of place cells when the mouse explores two different environments. **d**. Quantification of place field stability by correlation analyses in the three situations shown in panels **a—c**: Sleep pairing: correlation of firing maps obtained in exploration sessions performed before and after the sleep—pairing procedure (panel **a**); Wake pairing: correlation of firing maps obtained before and during the wake—pairing procedure (panel b); Control remapping session: correlation of firing maps obtained in two different environements (panel **c**). (Mann & Whitney, Sleep—pairing session vs. Control remapping session, n=11, n=5, Z=2.77, P=0.005; Wake Pairing session vs. Control remapping session n=10, n=5, Z=2.59, P=0.0094; Sleep Pairing session vs. Wake Pairing session n=11, n=10, Z=0.53, P=0.59). ** P <0.01 , NS: non significant.

e—f. Instantaneous phase distribution of theta filtered LFP 500ms before MFB stimulations trains and 500ms after stimulation artifacts, with stimulation either triggered manually during the classical place preference (**e**) or by a theta modulated place cell during wake—pairing protocol (**f**). For phase and kappa value, black and red dots indicate a significant locking of the phase (different from random phase distribution). The p value corresponds to the statistical difference between the observed distribution of the phases of the LFP filtered in the Theta band before and after the stimulation and a uniform circular distribution.

These panels show that in our conditions, MFB stimulation did not modify theta oscillations during exploration. This is an important control since stimulations in the hypothalamic region can drive (or reset) theta oscillations[22,23], Also MFB stimulation delivered either during sleep— or wake—pairing protocols, induced no modification of the place fields' properties, as correlations were significantly higher compared to an additional session where mice are placed in two different environments causing place cells remapping. Finally, these panels must be related to the main result of the paper: rewarding stimulations triggered by spikes of a place cell could induce place preference (Fig. 2a), further supporting the absence of modification of place fields by MFB stimulations as previously observe by Kobayashi and colleagues[15].

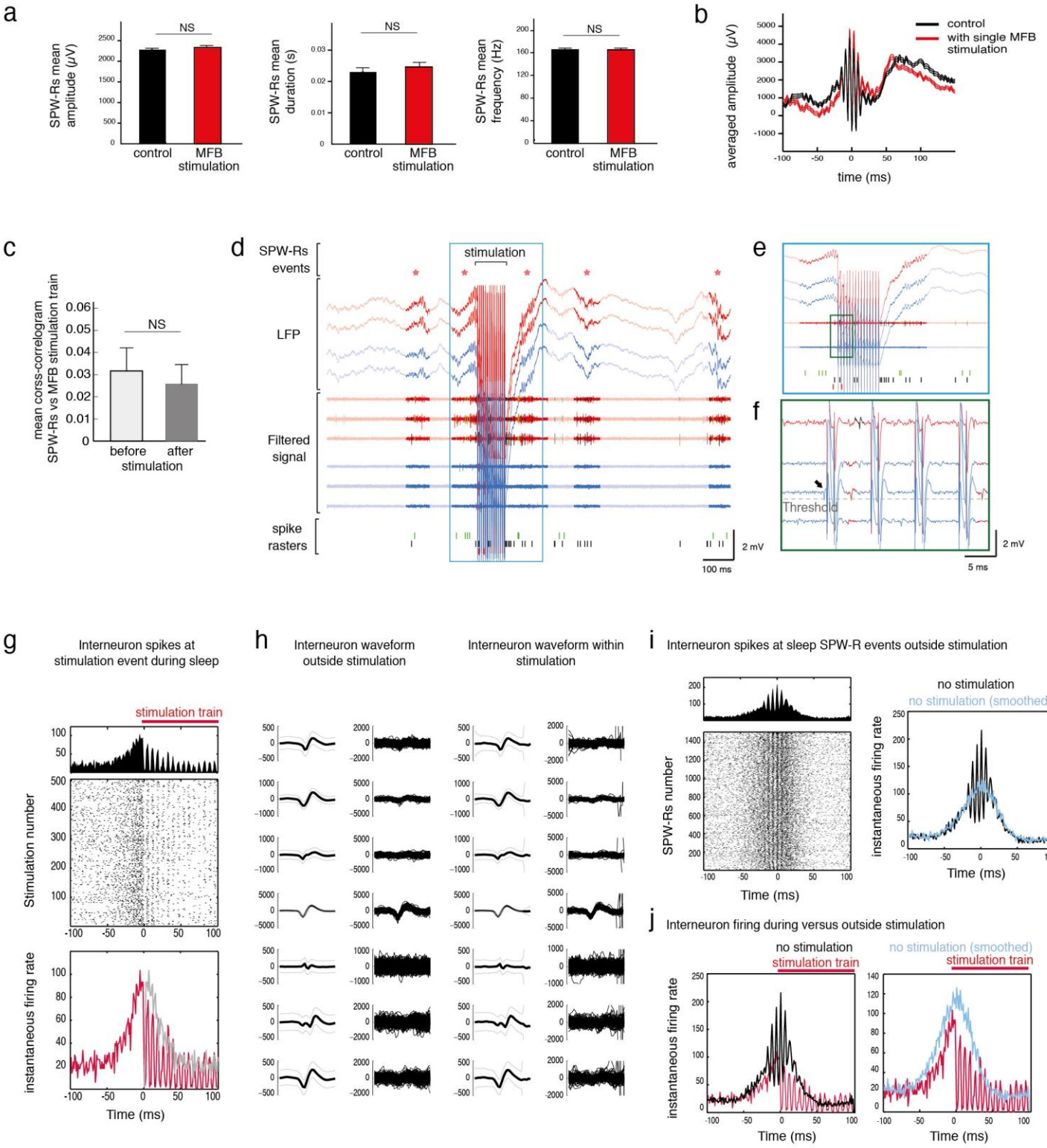

Nature Neuroscience: doi:10.1038/nn.3970

Supplementary Figure 4

MFB stimulation does not alter sleep sharp-wave ripples (SPW-Rs), nor associated neuronal activity.

a. Sleep SPW—Rs mean amplitude, duration and frequency with co—occurrence of a single MFB stimulation (red) or without (black). Wilcoxon matched pairs test, SPW—Rs with stimulation: n=35, SPW—Rs without stimulation: n=41; Amplitude, Z=1.20, P=0.30, Duration: Z=1.20, P=0.22, Frequency: Z=0.98, P=0.31. **b**. Averaged hippocampal LFP at time of SPW—Rs with concomitant single MFB stimulation after removal of the stimulation artifact (red) or without (black). **c**. Cross—correlogram between SPW—Rs and MFB Stimulation train, averaged on 3s before or after stimulation (Wilcoxon matched pairs test, n=5, Z=1.21, P=0.22). **d**. Representative recording period of selected channels from two stereotrodes (red and blue) within hippocampal pyramidal layer during a train of MFB stimulation. From top to bottom: Raw data, filtered signal (> 600 Hz) with colored spikes and raster plot of offline—clustered neurons. Red stars indicate SPW—R events. The MFB stimulation train does not preclude burst of ripples classically observed. **e**. High magnification of the stimulation train. Ripple—related spiking activity is not affected by MFB stimulation train as assessed by the presence of the interneuron's spikes (black raster) during the stimulation train. **f**. Higher magnification within the stimulation train. Note the presence of the spike crossing the threshold (dashed line) that triggered the MFB stimulation train (black arrow, spike could not be clustered offline due to stimulation artifact) and during the stimulation train (red spikes on blue traces).

g. Top: PETH centered on the start of MFB stimulation train (red bar) and spikes raster plot of the interneuron displayed in black in the raster shown in panel **d**. Bottom: Same PETH superimposed with the symmetric trace of the pre— stimulation train period (grey). **h**. Mean +/—SEM (left) and superimposition of waveforms (right) of the same interneuron's spikes on seven channels of an octrode, during sleep outside (left panel) or within (right panel) train of MFB stimulation. **i**. Left: SPW—Rs centered PETH and raster of the same interneuron spikes during sleep without MFB stimulation. Right: same PETH without (black) or with an additional jitter that smoothes oscillating firing during SPW—Rs (blue). **j**. Superimposition of the raw (left panel, black) or smoothed (right panel, blue) SPW—Rs centered PETH (as in panel **i**) to the stimulation centered PETH (as in panel **g**, red).

NS: non significant. Error bars indicate SEM.

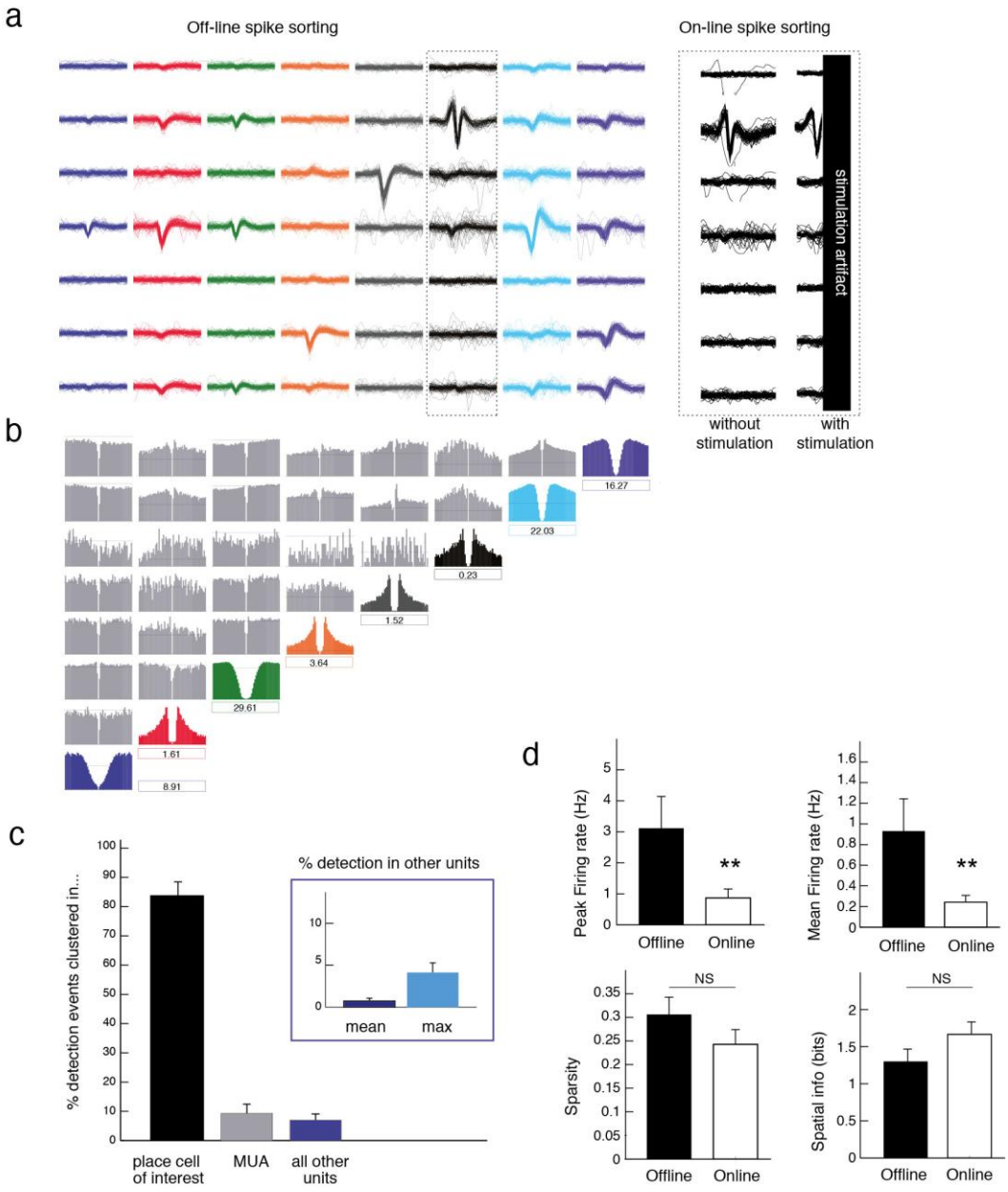

Supplementary Figure 5

Offline spike sorting and online spike detection.

a. Comparison between offline clustering and online voltage threshold—based spike sorting. Each column corresponds to the respective waveforms of eight hippocampal neurons recorded from one stereotrode and isolated by offline automatic clustering. The dashed squares emphasize that spikes detected online correspond to the black waveform without ambiguity. MFB stimulation automatically triggered by spike detection causes an electrical artifact that prevents the recording of the end of the waveform. **b**. Cross—correlograms (grey) and autocorrelogramms (color) of the same eight neurons as in panel a. Mean firing rates (Hz) are indicated underneath each autocorrelogram. **c**. Specificity quantification of online spike sorting compared to offline clustering for all

pairing protocols (sleep and wake). Percentage of detected events categorized into a unique cluster corresponding to the selected place cell (black), into multi—unit activity (MUA, grey), or into other (erroneous) clusters (blue). Insert: detail analysis of clusters containing misassigned spikes. For all sessions: mean percentage of detected spikes in each erroneous cluster and maximum percentage of detected spikes found over all erroneous clusters. Note that among all spikes detected online, offline clustering shows that 80% of them belonged to the cluster of the place cell of interest whereas less than 10% were clustered into multi—unit activity. Multi—unit cluster mostly corresponds to the spikes of the place cell of interest, to very few noisy signal and spikes of other units. For all recording sessions, on average, 1% of the detection events corresponded to other clustered cells. For each animal, the cluster with the maximum of misassigned spikes represented on average 5% of all detected events, meaning that a maximum of 5% of the MFB stimulations were paired to a different neuron. **d**. Characterization of the cells used in the pairing protocols (n=10) when detected online versus clustered offline in terms of firing rate (Wilcoxon matched pairs test, n=10, Z=2.8, P=0.005), sparsity (Wilcoxon matched pairs test, Z=1.58, P=0.11) and spatial information (Wilcoxon matched pairs test, Z=1.27, P=0.20). Note that sparsity and spatial information were similar for the place cells detected with online and offline methods, whereas there is a decrease in peak and mean firing rate obtained with the online method, consistent with the absence of detection of lower spikes during burst of complex spikes cells. Mean correlation between firing maps for online and offline detected spikes was 0.80+/—0.12.
** P <0.01, NS: non significant.

a

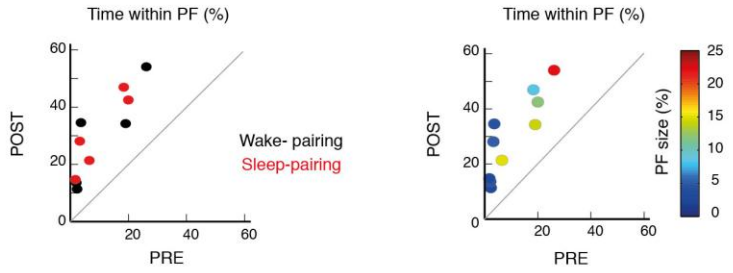

b

	Sleep-pairing	Sleep-pairing	control wake-pairing
	PRE vs theoretical random p values exploration	PRE vs POST p values	PRE vs stimulation p values
Excluded mice	0.18 0.30	0.14 0.41	1 0.43
Included mice	0.64 0.55 0.47 0.11 0.98	0.013 0.015 0.010 0.001 8.61e-05	1.51e-08 4.30e-05 2.38e-06 0 1.22e-09

c

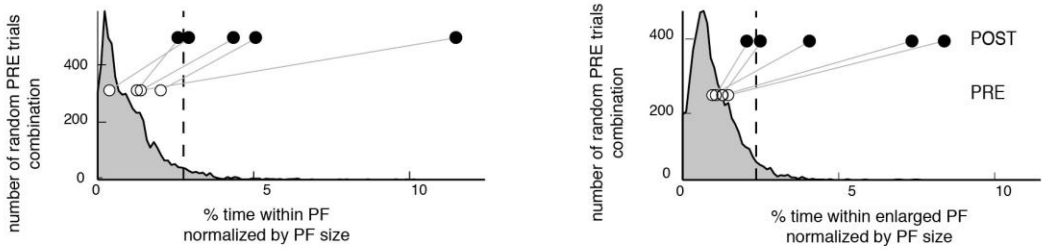

Supplementary Figure 6

Additional statistical quantification of the place preference induced by the sleep-pairing protocol.

a. Left. Correlation between PRE and POST sessions of sleep—pairing (n=5, red dots) or wake—pairing (n=5, black dots) protocols, in term of percentages of time spent in PF. Note that POST values are always bigger than PRE. Right. Correlation between PRE and POST sessions of those same sleep— and wake—pairing experiments, color scale corresponds to the percentage of the exploring area occupied by the PF. **b**. Table with exhaustive Khi2 proportion comparison between proportion of time spent inside and outside the place fields (PF) in PRE and POST session of sleep—pairing protocol (2nd column) or between PRE and stimulation sessions of the control wake—pairing protocol (3rd column), see Figure 3c for bar representation. First column corresponds to the comparison between proportion of time spent in the PF in PRE session of sleep—pairing protocol and the theoretical proportion of time spent in the PF according to PF size in case of random exploration (see Online Methods for details). On the basis of the significance in 3rd column, animals were either included (n=5) or excluded (n=2), see exclusion criterion 3. **c**. Distribution of percentage of time spent in PF (normalized by PF size) for random combination of 4 trials (out of 8) obtained from PRE sessions of all protocols (sleep—pairing protocol, wake—pairing protocol and classical place preference). Grey area represents the generated distribution, with the values of PRE sessions (white dots) and POST sessions (black dots) of the sleep—pairing protocol displayed on top of it. Dotted line represented the 95th percentile. Four of the 5 mice of the sleep—pairing protocol stood in the 5% extreme part of the distribution (the last one was at the 93th percentile). Left. Distribution computed by using time spent in PF, not significantly different from a homogenous exploration of the environment (see Online Methods), for which the normalized value is 1 (student t test, n=5914, P=0.47). Right. Same result is obtained by using time spent in the enlarged PF (student t test, n=5914, P=0.96).

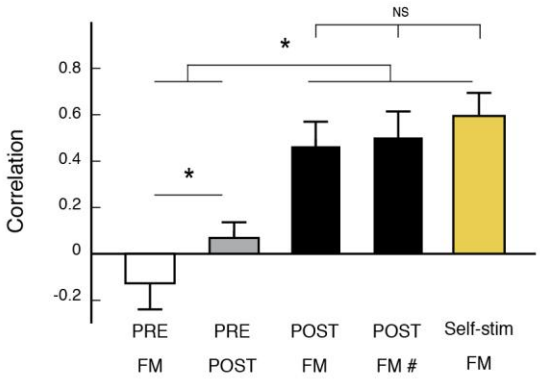

Supplementary Figure 7

Partial correlations of occupancy and firing map before, during and after wake-pairing protocol.

Correlation of occupancy maps in PRE versus POST wake pairing session (grey), or correlation between detected place cell's firing map (FM) and occupancy map in PRE and POST wake pairing session, or during wake pairing (self—stim) sessions (Friedman test, khi2=16.16 (n=5,df=4) *P=0.0023). Correlation with FM is increased during POST (n=5, correlation PRE/FM vs. POST/FM, Wilcoxon matched pairs test, Z=2.02, *P=0.043, correlation PRE/POST vs. POST/FM, Wilcoxon matched pairs test, Z=2.02, *P=0.043, correlation PRE/FM vs. PRE/POST, Wilcoxon matched pairs test, Z=2.02, *P=0.043). Same results were observed with partial correlation (#) between POST occupancy map and FM when corrected by PRE occupancy map (n=5, correlation PRE/FM vs. POST/FM corrected from PRE Wilcoxon matched pairs test, Z=2.02, *P=0.043, correlation POST/FM vs. POST/FM corrected from PRE, Wilcoxon matched pairs test, Z=1.21, P=0.22). Interestingly, this positive correlation is comparable to the one seen during the control wake—pairing session, where the mouse is actually self—stimulating (yellow, as in fig.2e) (PRE/FM vs. self—stim/FM: Wilcoxon matched pairs test, Z=2.02, *P=0.043, POST/FM vs. self—stim/FM, Wilcoxon matched pairs test, Z=1.21, P=0.22, self—stim/FM vs. POST/FM corrected from PRE Wilcoxon matched pairs test, Z=0.13, P=0.89). Note the absence of correlation in PRE sessions excluding a bias of behavior induced by arena properties. NS: not significant.

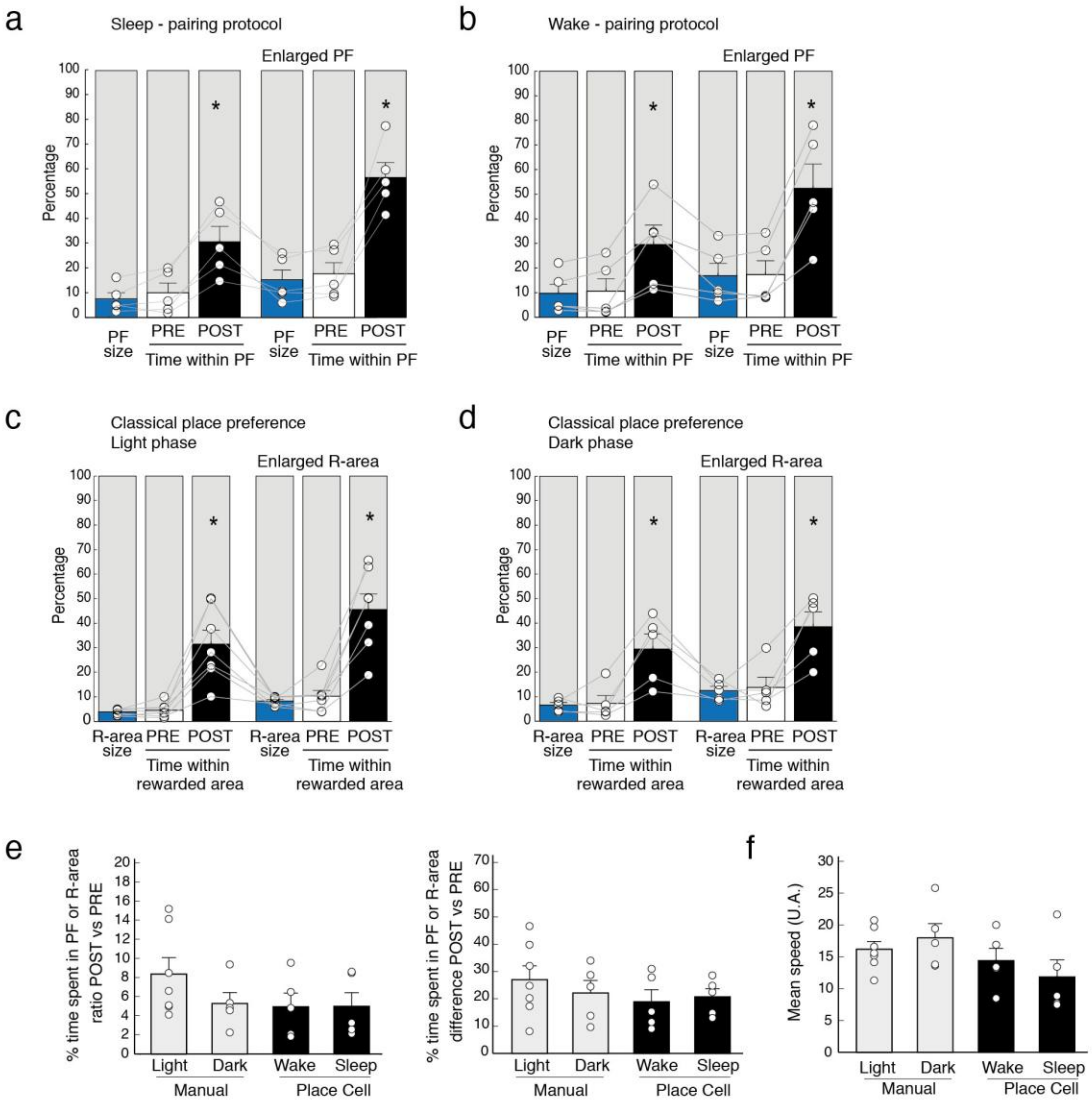

Supplementary Figure 8

Comparison between place preference tasks in all configurations and effect of the circadian rhythm.

a—b. Percentage of time spent within normal place field (left) or enlarged place field (right) in PRE and POST sessions of the sleep–pairing protocol (a, 12:00—15:00, n=5) or the wake—pairing protocol (b, 12:00—15:00, n=5). **c—d**. Percentage of time spent within rewarded area (R—area, left) or enlarged R—area (right) in PRE and POST sessions of the classical place preference using manual stimulation, induced either during the light phase (**c**, 12:00—15:00, n=7) or the dark phase (**d**, 0:00—3:00, n=5) of the day. Panels **a** to **d**, Wilcoxon matched pairs test, all comparison PRE vs. POST, **a—b,d**: n=5, Z=2.02, P=0.043; **c**: n=7, Z=2.37, P=0.018. *P <0.05.

e—f. Comparison of mouse behavior between place cell—stimulation pairing during sleep or wakefulness, with classical place preference (manual place—stimulation pairing) during light or dark phase for different parameters: **e**. Percentage of time spent in place field or rewarded area (R—area) in the POST session normalized by the PRE session, expressed either as a ratio POST/PRE (left, Kruskall Wallis, H(3,22)=3.27, P=0.35) or as a difference POST—PRE (right, Kruskall Wallis, H(3,22)=1.40, P=0.70). **f**. Mean running speed averaged in the different protocols (Kruskall Wallis, H(3,22)=4.279, P=0.23).

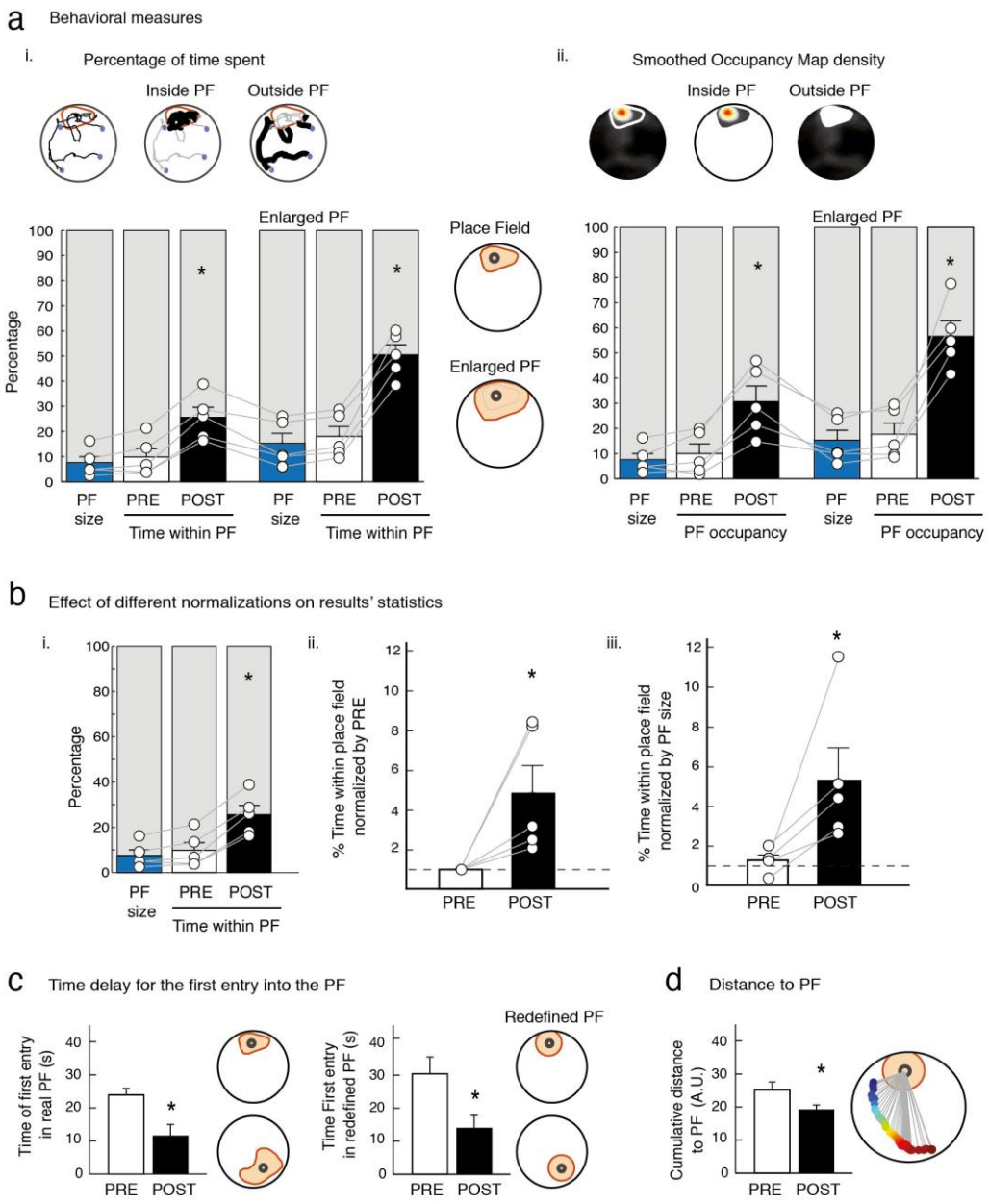

Supplementary Figure 9

Quantification of behavioral measures expressed in the sleep-pairing protocol (*n* = 5) and normalization methods.

a. Effect of the definition of the place field (PF). Percentage of time spent in PF (i) and density of occupation inside PF (ii) where "enlarged PF" corresponds to the PF artificially enlarged by the Matlab function imdilate. **b**. Time spent in PF during PRE and POST session, either not normalized (i, as in panel **a**), normalized by the time spent in PF during PRE (ii), or normalized by the PF size (iii). **c**. Time of first entry into PF in real place fields and in area of standardized size surrounding the center of PF. **d**. Cumulative distance to PF. **a—d**, Wilcoxon matched pairs test, all comparison PRE vs. POST, n=5, Z=2.02, P=0.043. * P <0.05.

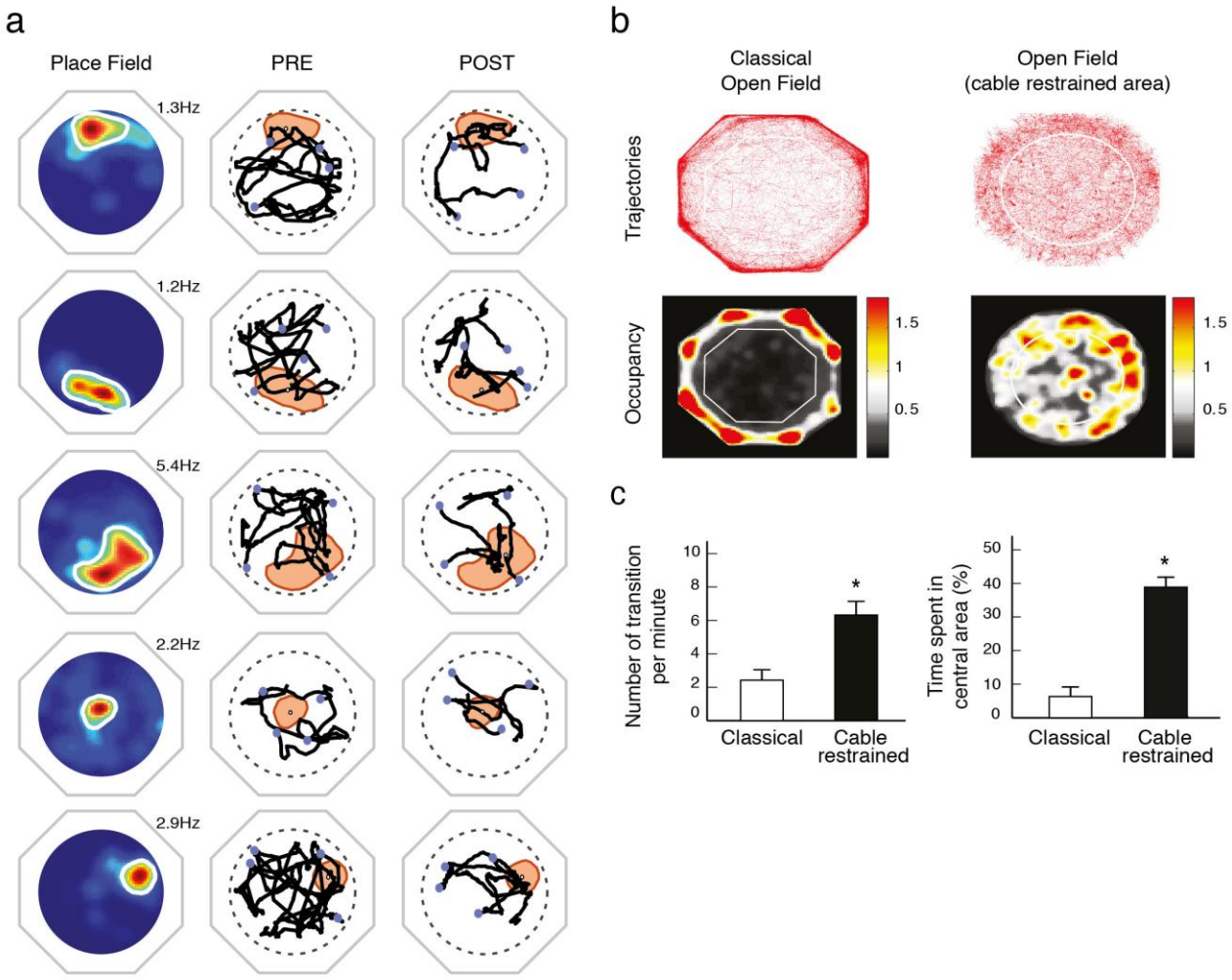

Supplementary Figure 10

Fine characterization of mouse behavior during experiments

Left. Raw trajectories before and after sleep learning

a. Left Column. Firing map with delimited place fields (white line) and maximum firing rate (Hz, red) of the detected place cells. Middle and Right columns. Trajectories during the 4 trials from PRE and POST sessions of the sleep pairing protocol for the five included mice. Blue dots correspond to starting points of each trial. Red areas correspond to place fields used for analysis.

Right. Homogenous exploratory behavior with cable—restrained method

b.Trajectories (up) and mean occupancy maps (bottom) exploration (30 minutes) in an octagonal classical open field (left) and in the same open field (identical shape and external clues) where exploration is restricted by the recording cable length (right). White lines represent central area, corresponding to 50% of the total reachable surface of the environment. **c**. Number of transitions per minute between central and external area (Wilcoxon matched pairs test, n=6, Z=2.20, P=0.027), and percentage of time spent within the central area (Wilcoxon matched pairs test, n=6, Z=2.20, P=0.027) over 30min—exploration in classical open field (white) versus cable—restrained exploration (black). Error bars indicate SEM.